

**Table.** Main characteristics of studies since 2010 about different algorithms for gait-event estimation using wearable inertial sensors. a: acceleration;  $\omega$ : angular rate; B: magnetic field. 1, 2, 3: number of sensor’s dimensions; HS: heel strike; TS: toe strike; HO: heel off; TO: toe off; c: comfortable; f: fast; s: slow; ?: not reported.

Ref.	Sensor	Number of subjects		Foot drop	Detected gait event				Algorithm	Real-time	Speeds
		Healthy	Impaired		HS	TS	HO	TO			
[1]	a <sup>3</sup>	6	-	-	✓	-	-	✓	Symbolization	?	c s
[2]	$\omega^1$	7	-	-	-	-	-	✓	Rule-based	-	c
[3]	a <sup>3</sup> $\omega^3$	-	1	✓	-	-	-	✓	Rule-based	Adjustable	c
[4]	a <sup>3</sup>	6	-	-	-	-	✓	-	Peak detection	✓	c f s
[5]	$\omega^1$	6	-	-	-	-	✓	✓	Hidden Markov models	-	c f s
[6]	$\omega^1$	10	10	-	✓	-	✓	-	Hidden Markov models	Adjustable	c f
[7]	a <sup>3</sup> $\omega^3$	10	32	-	✓	✓	✓	✓	Rule-based	Adjustable	c
[8]	a <sup>3</sup> $\omega^3$ B <sup>3</sup>	10	-	-	-	-	-	✓	Decision tree	Adjustable	c f
[9]	$\omega^1$	9	-	-	-	-	-	✓	Hidden Markov models	-	c f s
[10]	$\omega^1$	7	-	-	-	-	-	✓	Rule-based	-	c
[11]	$\omega^1$	10	-	-	✓	-	✓	-	Hidden Markov models	Adjustable	c
[12]	a <sup>3</sup>	10	10	-	-	-	-	✓	Rule-based	Adjustable	c
[13]	a <sup>3</sup> $\omega^3$ B <sup>3</sup>	10	30	-	✓	-	-	✓	Rule-based	-	c f
[14]	a <sup>3</sup> $\omega^3$	5	-	-	✓	-	-	✓	Rule-based	-	c f s
[15]	a <sup>3</sup> $\omega^3$ B <sup>3</sup>	7	1	-	✓	✓	✓	✓	Rule-based	✓	?
[16]	$\omega^3$	16	-	-	✓	-	-	✓	Rule-based	✓	C
[17]	a <sup>3</sup>	7	-	-	✓	✓	✓	✓	Rule-based	-	C
[18]	$\omega^1$	10	10	✓	-	✓	✓	-	Hidden Markov models	-	c s
[19]	a <sup>3</sup> $\omega^3$	14	5	✓	-	-	-	✓	Rule-based	✓	c f s
[20]	a <sup>3</sup> $\omega^3$ B <sup>3</sup>	10	-	-	✓	-	-	✓	Rule-based	-	C
[21]	a <sup>3</sup> $\omega^3$	10	32	-	✓	-	-	✓	Hidden Markov models/SVM	-	c f
[22]	a <sup>3</sup>	20	-	-	✓	-	-	✓	Time-frequency analysis	-	c f
[23]	a <sup>3</sup> $\omega^3$ B <sup>3</sup>	2	-	✓	✓	-	-	✓	Cycle-extremum/Threshold update	✓	?
[24]	a <sup>3</sup>	20	-	-	✓	-	-	✓	Rule-based	-	c f
[25]	a <sup>3</sup>	11	-	-	✓	-	-	✓	Rule-based	-	c f
[26]	a <sup>3</sup> $\omega^3$ B <sup>3</sup>	11	15	-	✓	-	-	✓	Peak detection	-	c
[27]	a <sup>3</sup> $\omega^3$ B <sup>3</sup>	57	-	-	✓	-	-	✓	Rule-based	✓	c

## References

- [1] A. Sant’Anna and N. Wickström, “A symbol-based approach to gait analysis from acceleration signals: Identification and detection of gait events and a new measure of gait symmetry,” *IEEE Transactions on Information Technology in Biomedicine*, 2010.
- [2] P. Catalfamo, S. Ghoussayni, and D. Ewins, “Gait event detection on level ground and incline walking using a rate gyroscope,” *Sensors (Basel)*, vol. 10, no. 6, pp. 5683–5702, 2010.
- [3] D. Kotiadis, H. J. Hermens, and P. H. Veltink, “Inertial Gait Phase Detection for control of a drop foot stimulator. Inertial sensing for gait phase detection,” *Medical Engineering and Physics*, 2010.
- [4] M. Patterson and B. Caulfield, “A novel approach for assessing gait using foot mounted accelerometers,” in *Proceedings of the 5th International ICST Conference on Pervasive Computing Technologies for Healthcare*, 2011.
- [5] A. Mannini and A. M. Sabatini, “Gait phase detection and discrimination between walking–jogging activities using hidden Markov models applied to foot motion data from a gyroscope,” *Gait & Posture*, 2012.
- [6] N. Abaid, P. Cappa, E. Palermo, M. Petrarca, and M. Porfiri, “Gait Detection in Children with and without Hemiplegia Using Single-Axis Wearable Gyroscopes,” *PLoS ONE*, 2013.
- [7] B. Mariani, H. Rouhani, X. Crevoisier, and K. Aminian, “Quantitative estimation of foot-flat and stance phase of gait using foot-worn inertial sensors,” *Gait and Posture*, 2013.
- [8] D. Novak *et al.*, “Automated detection of gait initiation and termination using wearable sensors,” *Medical Engineering and Physics*, 2013.
- [9] A. Mannini, V. Genovese, and A. M. Sabatini, “Online decoding of hidden markov models for gait event detection using foot-mounted gyroscopes,” *IEEE Journal of Biomedical and Health Informatics*, 2014.
- [10] P. C. Formento, R. Acevedo, S. Ghoussayni, and D. Ewins, “Gait event detection during stair walking using a rate gyroscope,” *Sensors (Switzerland)*, vol. 14, no. 3, pp. 5470–5485, 2014.
- [11] J. Taborri, S. Rossi, E. Palermo, F. Patanè, and P. Cappa, “A novel HMM distributed classifier for the detection of gait phases by means of a wearable inertial sensor network,” *Sensors (Switzerland)*, 2014.
- [12] J. Rueterbories, E. G. Spaich, and O. K. Andersen, “Gait event detection for use in FES rehabilitation by radial and tangential foot accelerations,” *Medical Engineering and Physics*, vol. 36, no. 4, pp. 502–508, 2014.
- [13] D. Trojaniello *et al.*, “Estimation of step-by-step spatio-temporal parameters of normal and impaired gait using shank-mounted magneto-inertial sensors: Application to elderly, hemiparetic, parkinsonian and choreic gait,” *Journal of NeuroEngineering and Rehabilitation*, 2014.
- [14] P. Fraccaro, L. Walsh, J. Doyle, and D. O’Sullivan, “Real-world Gyroscope-based Gait Event Detection and Gait Feature Extraction,” *eTELEMED 2014, The Sixth International Conference on eHealth, Telemedicine, and Social Medicine*, no. c, pp. 247–252, 2014.
- [15] B. Chen, E. Zheng, Q. Wang, and L. Wang, “A new strategy for parameter optimization to improve phase-dependent locomotion mode recognition,” *Neurocomputing*, vol. 149, no. PB, pp. 585–593, 2015.
- [16] D. Gouwanda and A. A. Gopalai, “A robust real-time gait event detection using wireless gyroscope and its application on normal and altered gaits,” *Medical Engineering and Physics*, vol. 37, no. 2, pp. 219–225, 2015.
- [17] M. Boutaayamou *et al.*, “Development and validation of an accelerometer-based method for quantifying gait events,” *Medical Engineering and Physics*, 2015.
- [18] J. Taborri, E. Scalona, E. Palermo, S. Rossi, and P. Cappa, “Validation of inter-subject training for hidden markov models applied to gait phase detection in children with Cerebral Palsy,” *Sensors (Switzerland)*, 2015.
- [19] P. Muller, T. Seel, and T. Schauer, “Experimental Evaluation of a Novel Inertial Sensor Based Realtime Gait Phase Detection Algorithm,” in *Proc. of the 5th European Conference on Technically Assisted Rehabilitation - TAR 2015*, 2015.
- [20] F. A. Storm, C. J. Buckley, and C. Mazzà, “Gait event detection in laboratory and real life settings: Accuracy of ankle and waist sensor based methods,” *Gait and Posture*, 2016.
- [21] A. Mannini, D. Trojaniello, A. Cereatti, and A. M. Sabatini, “A Machine Learning Framework for Gait Classification Using Inertial Sensors: Application to Elderly, Post-Stroke and Huntington’s Disease Patients,” *Sensors*, vol. 16, no. 2, p. 134, 2016.
- [22] S. Khandelwal and N. Wickström, “Gait Event Detection in Real-World Environment for Long-Term Applications: Incorporating Domain Knowledge Into Time-Frequency Analysis,” *IEEE Transactions on Neural Systems and Rehabilitation Engineering*, vol. 24, no. 12, pp. 1363–1372, 2016.
- [23] Y. Gao *et al.*, “A Novel Gait Detection Algorithm Based on Wireless Inertial Sensors,” *IFMBE Proceedings*, vol. 62, pp. 300–304, 2017.
- [24] S. Khandelwal and N. Wickström, “Evaluation of the performance of accelerometer-based gait event detection algorithms in different real-world scenarios using the MAREA gait database,” *Gait and Posture*, vol. 51, pp. 84–90, 2017.
- [25] S. Mo and D. H. K. K. Chow, “Accuracy of three methods in gait event detection during overground running,” *Gait and Posture*, vol. 59, pp. 93–98, 2018.
- [26] L. Carcreff *et al.*, “What is the best configuration of wearable sensors to measure spatiotemporal gait parameters in children with cerebral palsy?,” *Sensors (Switzerland)*, vol. 18, no. 2, p. 394, 2018.
- [27] S. Šprager and M. Jurič, “Robust Stride Segmentation of Inertial Signals Based on Local Cyclicity Estimation,” *Sensors*, vol. 18, no. 4, p. 1091, Apr. 2018.

### Information about the additional subject with foot drop gait abnormality in the open dataset

(<https://doi.org/10.6084/m9.figshare.7778255>)

One female subject with a foot drop gait abnormality voluntarily participated in this study. Her foot drop abnormality was at the left side of the body and it was caused by congenital cerebral palsy. At the time of evaluation, she was 25.2 years of age and had 50.0 kg of body mass, 161.0 cm of height, and 19.29 kg/m<sup>2</sup> of body-mass index. For this subject, there are data for 496 gait strides, with stride lengths varying from 1.03 m to 1.48 m and walking speeds varying from 0.85 m/s to 1.77 m/s. In the open dataset her data are identified as subject ‘00’ (the other subjects are identified from ‘01’ to ‘22’).

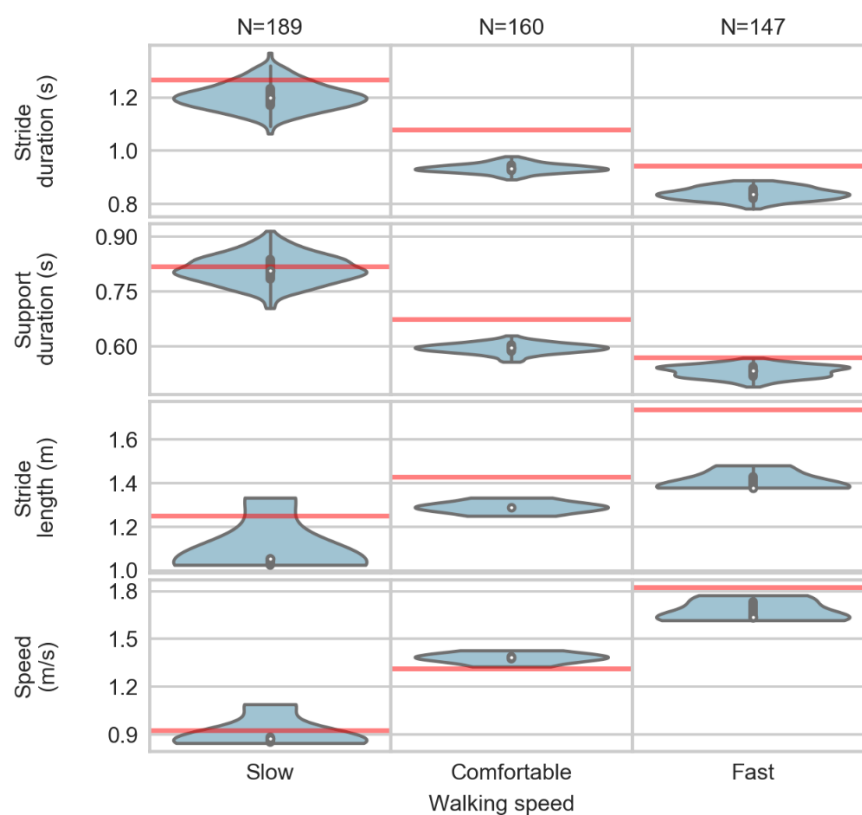


**Figure 1.** Violin plots (boxplots plus kernel density estimations) for the subject with foot drop from the open dataset for the gait variables: stride duration, support duration, stride length, and speed, calculated using the data from the force-sensitive resistor under the right foot for the different walking speeds. The numbers shown at the top of each column indicate the total number of gait strides available in the dataset at each speed (and used to generate these plots). For each variable, the curve represents an estimation of the data distribution, the vertical black line represents the interval for 95% of the data, the black box represents the interquartile range, and the central dot represents the median value. The horizontal red line represents the median value across the 22 healthy subjects.

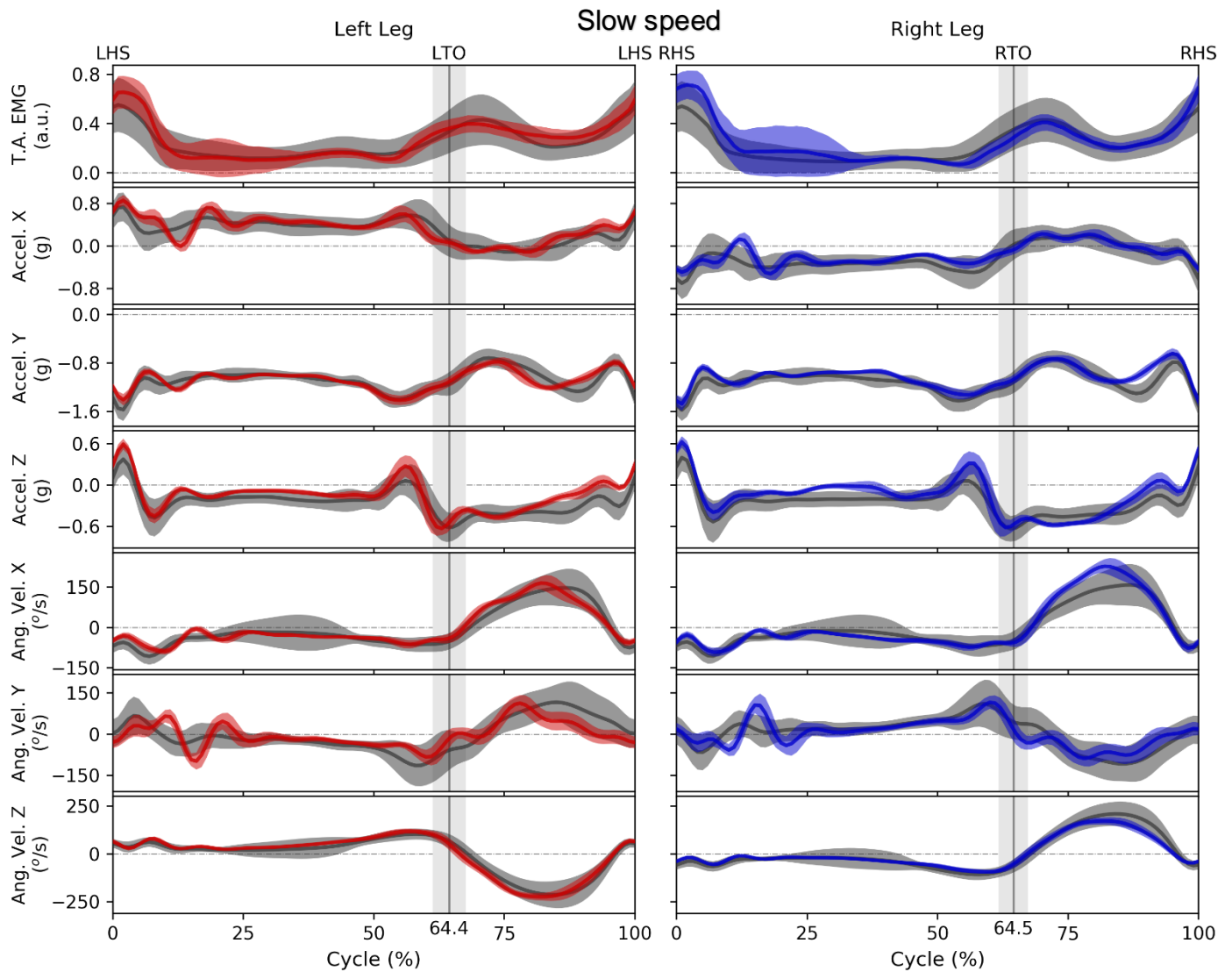


Figure 2. Mean  $\pm$  1 standard deviation for the subject with foot drop (red and blue) from the open dataset, compared to mean  $\pm$  1 standard deviation across the 22 healthy subjects (gray) for the measured signals: tibialis anterior electromyographic activity (EMG TA), three-dimensional acceleration (Accel.), and angular velocity (Ang. Vel.), over the left and right gait cycles walking at the slow speed (see article for the axes convention). The mean  $\pm$  1 standard deviation termination of the gait support phase, indicated by the LTO or RTO events, are shown by the vertical lines and shaded areas of the plots. The gait events were determined using the data from the force-sensitive resistor under the right and left feet. The abbreviations LHS, RHS, LTO, and RTO denote the gait events: left and right heel strike and left and right toe-off, respectively. These curves are based on a total of 160 gait strides.

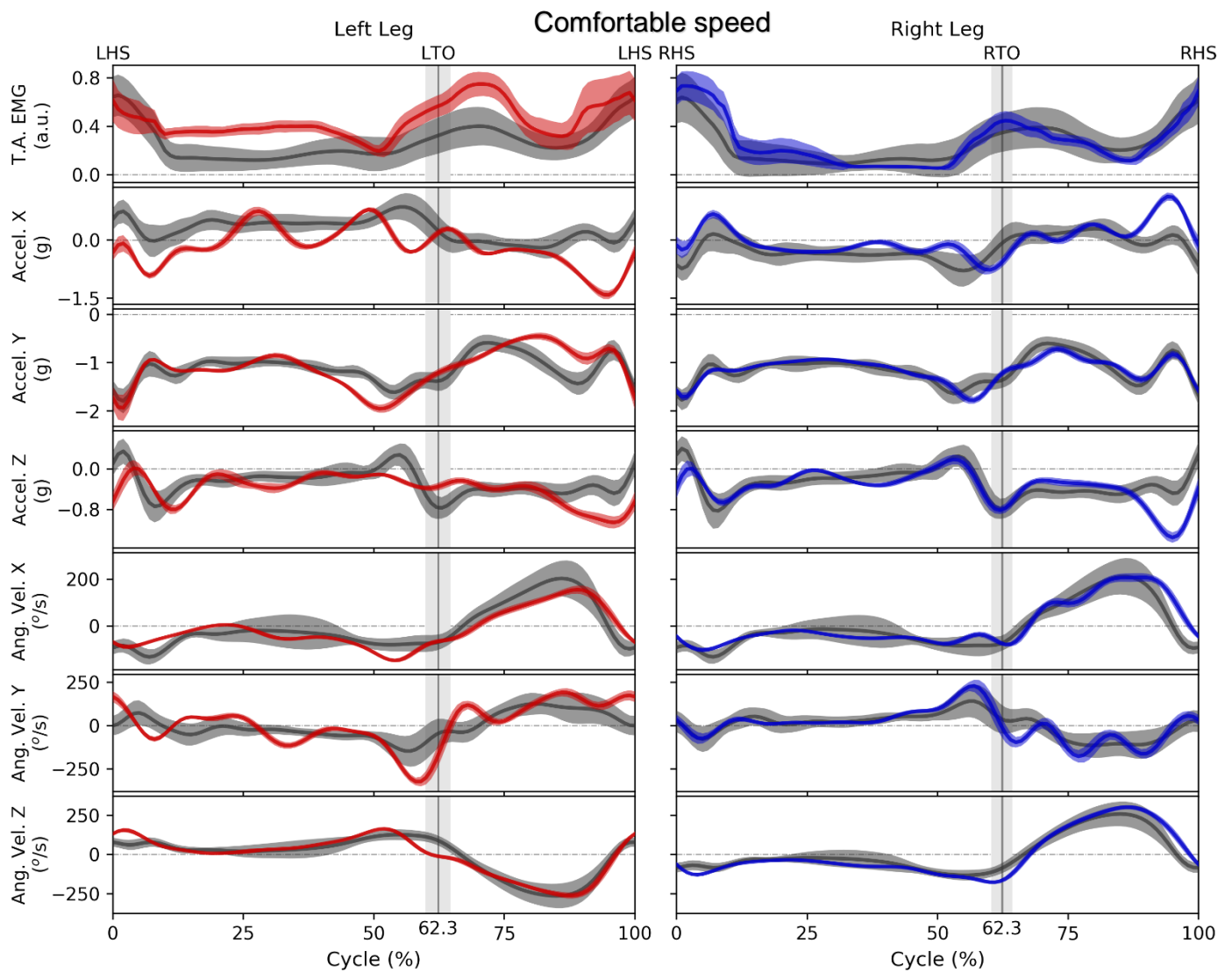


Figure 3. Mean  $\pm$  1 standard deviation for the subject with foot drop (red and blue) from the open dataset, compared to mean  $\pm$  1 standard deviation across the 22 healthy subjects (gray) for the measured signals: tibialis anterior electromyographic activity (EMG TA), three-dimensional acceleration (Accel.), and angular velocity (Ang. Vel.), over the left and right gait cycles walking at the comfortable speed (see article for the axes convention). The mean  $\pm$  1 standard deviation termination of the gait support phase, indicated by the LTO or RTO events, are shown by the vertical lines and shaded areas of the plots. The gait events were determined using the data from the force-sensitive resistor under the right and left feet. The abbreviations LHS, RHS, LTO, and RTO denote the gait events: left and right heel strike and left and right toe-off, respectively. These curves are based on a total of 160 gait strides.

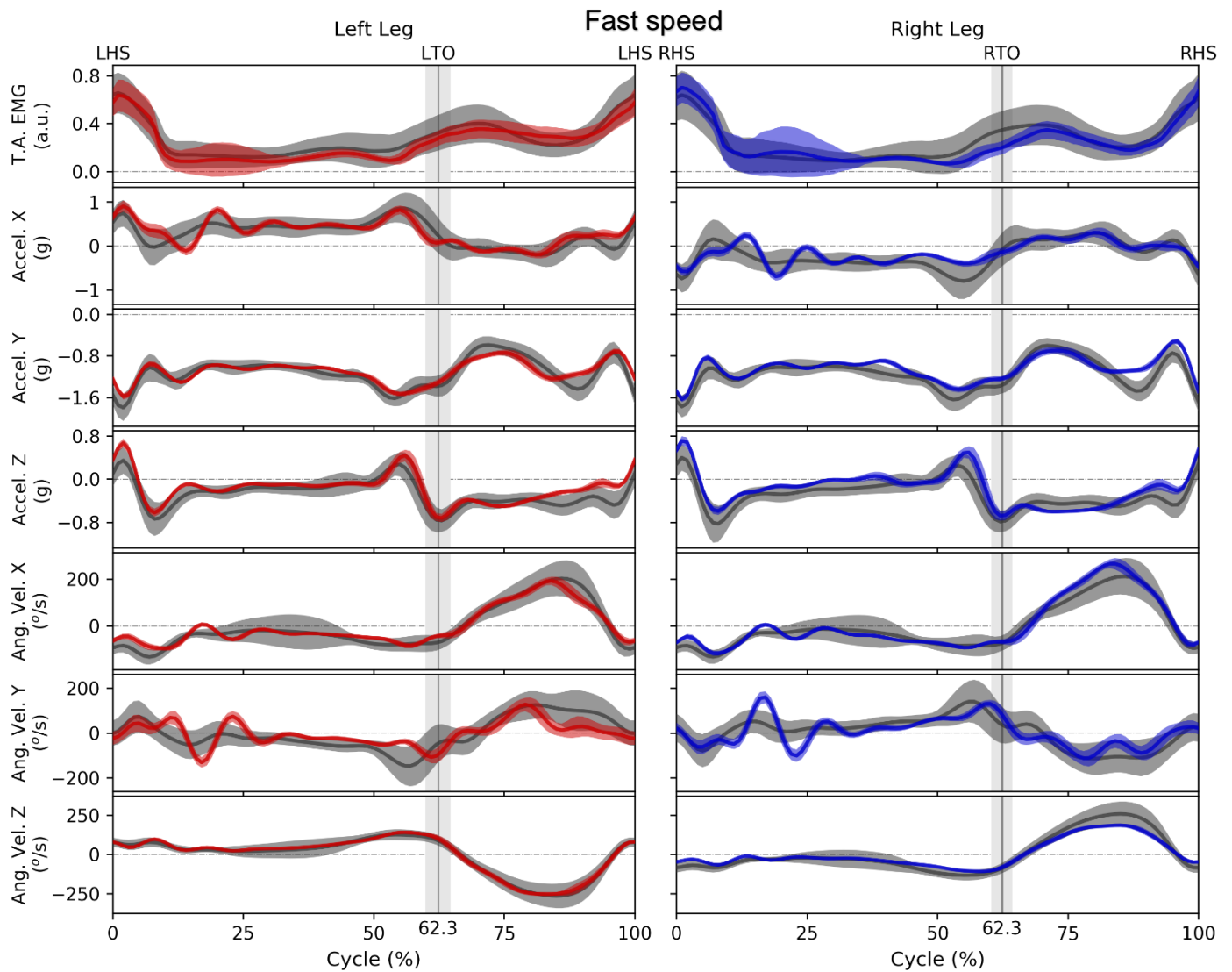


Figure 4. Mean  $\pm$  1 standard deviation for the subject with foot drop (red and blue) from the open dataset, compared to mean  $\pm$  1 standard deviation across the 22 healthy subjects (gray) for the measured signals: tibialis anterior electromyographic activity (EMG TA), three-dimensional acceleration (Accel.), and angular velocity (Ang. Vel.), over the left and right gait cycles walking at the fast speed (see article for the axes convention). The mean  $\pm$  1 standard deviation termination of the gait support phase, indicated by the LTO or RTO events, are shown by the vertical lines and shaded areas of the plots. The gait events were determined using the data from the force-sensitive resistor under the right and left feet. The abbreviations LHS, RHS, LTO, and RTO denote the gait events: left and right heel strike and left and right toe-off, respectively. These curves are based on a total of 160 gait strides.